

# Hot Electroweak Matter Near to the Critical Higgs Mass<sup>1</sup>

M. Gürtler<sup>1</sup>, E.-M. Ilgenfritz<sup>2, 3</sup>, A. Schiller<sup>1</sup>, C. Strecha<sup>1</sup>

<sup>1</sup> Institut für Theoretische Physik, Universität Leipzig, D-04109 Leipzig, Germany

<sup>2</sup> Institut für Physik, Humboldt-Universität, D-10115 Berlin, Germany

<sup>3</sup> Institute for Theoretical Physics, Kanazawa University, Kanazawa 920, Japan

**Abstract:** We discuss the end of the first order phase transition and the bound state spectrum, both at weak transition and at the crossover.

## 1 Introduction

Two years ago [1], we have presented here first results of our group obtained within the 3D approach, comparing the properties of the thermal phase transition in the  $SU(2)$  Higgs model at small coupling (Higgs mass)  $M_H^* = 35$  GeV with a more realistic  $M_H^* = 70$  GeV.<sup>2</sup> The endpoint of the phase transition and the physics near to the corresponding temperature  $T_c(m_H^{crit})$  is the topic of this talk.

In the meantime, due to efforts of three groups [3, 4, 2] using the 3D approach, various aspects of the high temperature electroweak phase transition (as latent heat and interface tension) have been explored in this model within this span of Higgs masses where the character of the transition changes drastically. The accuracy is inaccessible to 4D Monte Carlo simulations [5], although the results are consistent with each other where they can be compared [6, 7].

The interest in the properties of this phase transition resulted from the hope to work out - within the standard model - a viable mechanism for the generation of baryon asymmetry of the universe at the electroweak scale (see Z. Fodor [8]). It turned out, however, that in the case of the standard model, taking the lower bound of the Higgs mass into account, it is at most weakly first order. Together with the small amount of CP violation in the standard model this has ruled out the most economic scenario of BAU generation.

Using dimensional reduction [9] the simplest effective 3D  $SU(2)$  Higgs theory has the action

$$S_3 = \int d^3x \left( \frac{1}{4} F_{\alpha\beta}^b F_{\alpha\beta}^b + (D_\alpha \phi)^+ (D_\alpha \phi) + m_3^2 \phi^+ \phi + \lambda_3 (\phi^+ \phi)^2 \right) \quad (1)$$

<sup>1</sup>Talk at Buckow Symp. 97 given by E.-M. Ilgenfritz, supported by DFG under grant Mu932/1-4

<sup>2</sup> $M_H^*$ , together with the 3D gauge coupling, is labelling our lattice data. For relation to the zero-temperature Higgs mass, see Ref. [2].

with dimensionful, renormalisation group invariant couplings  $g_3^2$  and  $\lambda_3$  and a running mass squared  $m_3^2(\mu_3)$ . It is related to the corresponding lattice model with the action

$$S = \beta_G \sum_p \left(1 - \frac{1}{2} \text{tr} U_p\right) - \beta_H \sum_{x,\alpha} \frac{1}{2} \text{tr}(\Phi_x^+ U_{x,\alpha} \Phi_{x+\alpha}) + \sum_x (\rho_x^2 + \beta_R(\rho_x^2 - 1)^2) \quad (2)$$

and  $\rho_x^2 = \frac{1}{2} \text{tr}(\Phi_x^+ \Phi_x)$  through the following relations (clarifying the meaning of  $M_H^*$ )

$$\beta_G = \frac{4}{ag_3^2}, \quad \beta_R = \frac{\lambda_3 \beta_H^2}{g_3^2 \beta_G} = \frac{1}{8} \left(\frac{M_H^*}{80 \text{ GeV}}\right)^2 \frac{\beta_H^2}{\beta_G}, \quad \beta_H = \frac{2(1 - 2\beta_R)}{6 + a^2 m_3^2}. \quad (3)$$

The coupling parameters in the lattice action can be expressed in terms of  $4D$  couplings and masses. The bare mass squared is related to the renormalised  $m_3^2(\mu_3)$  (we choose  $\mu_3 = g_3^2$ ) through a lattice two-loop calculation [10]. Most of the  $3D$  numerical investigations have been done for the  $SU(2)$  Higgs model. The results obtained in the  $3D$  approach indicate the validity of the dimensional reduction near to the transition temperature for Higgs masses between 30 and 100 GeV.

Our simulations have been done on the DFG-sponsored Quadrics QH2 in Bielefeld, on a CRAY-T90 and a Quadrics Q4 at HLRZ in Jülich. Algorithmic details are described in Ref. [2]. In the course of time, we have explored the parameter range  $M_H^* = 35, 57, 70, 74, 76, 80$  GeV, looking for the strength of the transition, checking the approach to the continuum limit by varying  $\beta_G = 8, 12, 16 \propto 1/a$  and comparing with perturbation theory. The simulations at the last three parameter values  $M_H^*$  have been devoted exclusively to locate the endpoint of the transition line [11] in the  $m_H - T$  plane. The lattice size usually varied from  $20^3$  to  $80^3$ . In order to unambiguously locate the critical Higgs mass we had to increase the lattice to  $96^3$  simulating at  $M_H^* = 74$  GeV, the nearest to the critical value.

It has been essential to make extensive use of the Ferrenberg-Swendsen multihistogram technique. Data obtained at various  $M_H^*$  and  $\beta_H$  have been subject to global analysis by reweighting to other values, eventually extending the hopping parameter to complex values. The method constructs an optimal estimator of the spectral density of states (at fixed  $L$  and  $\beta_G$ ) occurring in the representation of the partition function

$$Z(L, \beta_G, \beta_H) = \int dS_1 dS_2 D_L(S_1, S_2, \beta_G) \exp\left(L^3(\beta_H S_1 - \beta_H^2 S_2)\right) \quad (4)$$

from the *measured* double-histograms in the two variables

$$S_1 = 3 \sum_{x,\alpha} \frac{1}{2} \text{tr}(\Phi_x^+ U_{x,\alpha} \Phi_{x+\alpha}), \quad S_2 = \frac{\lambda_3}{g_3^2 \beta_G} \left(\sum_x \rho_x^4 - 2 \sum_x \rho_x^2\right). \quad (5)$$

## 2 Finding $m_H^{crit}$

We have employed two methods to localise the critical Higgs mass. First we tried an interpolation of the discontinuity

$$\Delta\langle\phi^+\phi\rangle/g_3^2 = 1/8 \beta_G \beta_H \Delta\langle\rho^2\rangle, \quad (6)$$

based on reweighting simulation data taken at  $M_H^* = 70, 74$  and  $76$  GeV, in order to see where this turns to zero. This discontinuity is directly related to the latent heat. The pseudocritical  $\beta_{Hc}$  has been defined in two ways, by the maximum of the  $\rho^2$  susceptibility and by the minimum of the  $\rho^2$  Binder cumulant. For each  $M_H^*$ , an infinite volume extrapolation must be performed. For this purpose we have expressed the *physical* lattice size by the dimensionless variable  $Lag_3^2 = 4L/\beta_G$ . We have collected data from different lattice volumes  $L^3$ , from different  $\beta_G$  ( $= 12$  and  $16$ ) as well as from different definitions of  $\beta_{Hc}$  and found them scattered along a unique function of this variable (Fig. 1). We tried to fit the finite volume scaling behaviour

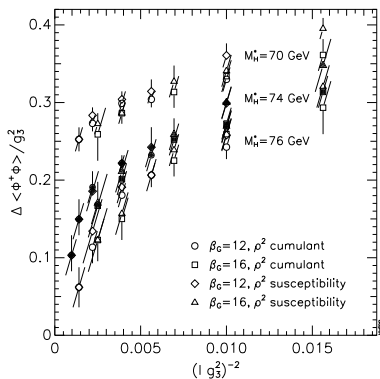


Figure 1: Thermodynamical limit for  $\Delta\langle\phi^+\phi\rangle$  at three  $M_H^*$  values (here  $l = aL$ )

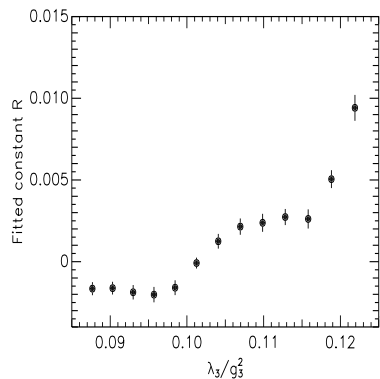


Figure 2: Minimal distance  $R$  of LY zeroes from real axis as function of  $\lambda_3/g_3^2$

as  $\Delta\langle\phi^+\phi\rangle_\infty - \Delta\langle\phi^+\phi\rangle_L \propto (L a g_3^2)^{-2}$  suggested by the Potts model. Using only the largest lattice volumes available, the criterion of vanishing latent heat gives an upper bound  $\lambda_3^{crit}/g_3^2 < 0.107$  for the existence of a first order transition.

The other method detects the end of the transition line using the finite size analysis of the Lee–Yang zeroes. A genuine phase transition is characterised by *non-analytical* behaviour of the infinite volume free energy density. This is caused by zeroes of the partition function (in our case as function of  $\beta_H$  extended to complex values) clustering along a line nearest to the real axis and pinching in the thermodynamical limit. If there is a first order phase transition the first few zeroes are expected at

$$\text{Im}\beta_H^{(n)} = \frac{2\pi\beta_{Hc}}{L^3(1+2\beta_{Rc})\Delta\langle\rho^2\rangle} \left(n - \frac{1}{2}\right), \quad \text{Re}\beta_H^{(n)} \approx \beta_{Hc}. \quad (7)$$

The partition function for complex couplings is obtained by reweighting from measurements at real couplings. The first zeroes can be well localised using the Newton-Raphson algorithm. We fit the imaginary part of the first zero for each available length  $Lag_3^2$  according to  $\text{Im}\beta_H^{(1)} = C(Lag_3^2)^{-\nu} + R$ . The scenario suggested is the change of the first order transition into an analytic crossover above  $M_H^{*crit}$ . A *positive*  $R$  signals that the first zero does not approach the real axis in the thermodynamical limit. A similar investigation has been performed recently at smaller gauge coupling in Ref. [12]. The fitted  $R$  crosses zero (Fig. 2) at  $\lambda_3^{crit}/g_3^2 = 0.102(2)$ . This

corresponds to a zero temperature Higgs mass  $m_H^{crit} = 72.4(9)$  GeV, and the phase transition line ends at a temperature of  $T_c = 110(1.5)$  GeV. This refers to the experimental top mass. For the purely bosonic Higgs model we get  $m_H^{crit} = 67.0(8)$  GeV and  $T_c = 154.8(2.6)$  GeV.

### 3 Bound states below and above $m_H^{crit}$

To study the ground *and* excited bound states with given  $J^{PC}$  one has to use cross-correlations between operators  $\mathcal{O}_i$  forming a complete set in that channel. They describe a spectral decomposition  $\Psi_i^{(n)} = \langle \text{vac} | \mathcal{O}_i | \Psi^{(n)} \rangle$  with  $|\Psi^{(n)}\rangle$  being the (zero momentum) energy eigenstates. According to the transfer matrix formalism, the connected correlation matrix

$$C_{ij}(t) = \langle \mathcal{O}_i(t) \mathcal{O}_j(0) \rangle = \sum_{n=1}^{\infty} \Psi_i^{(n)} \Psi_j^{(n)*} e^{-m_n t} \quad (8)$$

at time separation  $t$  gives the masses *and* wave functions.

Practically, only a *truncated* set of operators  $\mathcal{O}_i (i = 1, \dots, N)$  is used assuming that this allows to find the *lowest* states from the eigenvalue problem for  $C_{ij}(t)$ . However, truncation errors are not small. Solving instead the generalised eigenvalue problem

$$\sum_j C_{ij}(t) \Psi_j^{(n)} = \lambda^{(n)}(t, t_0) \sum_j C_{ij}(t_0) \Psi_j^{(n)} \quad (9)$$

these errors can be kept minimal ( $t > t_0, t_0 = 0, 1$ ) [13].

The wave function of state  $n$  at fixed small time  $t > t_0$  is found to be  $\Psi_i^{(n)}(t) = \langle \text{vac} | \mathcal{O}_i e^{-Ht} | \Psi^{(n)} \rangle$ . The components in the operator basis characterise the coupling of  $\mathcal{O}_i$  to the (ground or excited) bound state  $n$  in the  $J^{PC}$  channel. The masses of these states are obtained fitting the diagonal elements  $\mu^{(n)}(t)$

$$\mu^{(n)}(t) = \sum_{ij} \Psi_i^{(n)*} C_{ij}(t) \Psi_j^{(n)} \quad (10)$$

to a cosh form with  $t$  in some plateau region. In contrast to a blocking procedure used in [14], our base is built by a few types of gauge invariant operators  $\mathcal{O}_i$ , properly chosen with respect to lattice symmetry and quantum numbers, having different well-defined transverse extensions. In the Higgs channel ( $0^{++}$ ) we use the operators  $\rho_x^2$  and  $S_{x,\mu}(l) = \frac{1}{2} \text{tr}(\Phi_x^+ U_{x,\mu} \dots U_{x+(l-1)\mu,\mu} \Phi_{x+l\mu})$  as well as quadratic Wilson loops of size  $l \times l$ , in the  $\bar{W}$ -channel ( $1^{--}$ ) the operators  $V_{x,\mu}^b(l) = \frac{1}{2} \text{tr}(\tau^b \Phi_x^+ U_{x,\mu} \dots U_{x+(l-1)\mu,\mu} \Phi_{x+l\mu})$  and in the  $2^{++}$  channel  $S_{x,\mu}(l) - S_{x,\nu}(l)$  where  $l$  expresses the operator extension in lattice units. In our procedure, the operator  $\Phi^{(n)}$  projecting maximally onto state  $n$  is a optimised superposition  $\Phi^{(n)} = \sum_1^N a_i^{(n)} \mathcal{O}_i$  with coefficients provided by the (properly normalised) solutions  $\Psi_i^{(n)}$  of the generalised eigenvalue equation. The coefficients give direct access to the spatial extension of the states under study. This construction, at different  $\beta_G$ , should reveal the same wave function in position space as function of  $lag_3^2$ .

As examples we present in Figs. 3,4 squared wave functions in the  $0^{++}$  channel vs.  $lag_3^2$  near the end of the phase transition at  $M_H^* = 70$  GeV (from a  $30^3$  lattice). In the symmetric phase the second excitation is a pure  $W$ -ball state in agreement

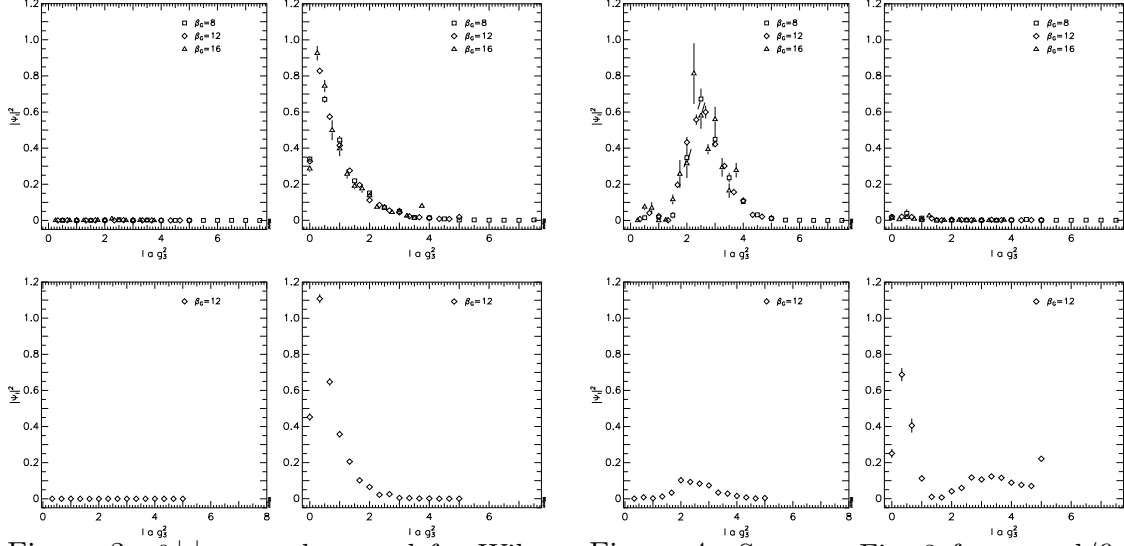


Figure 3:  $0^{++}$  ground state, left: Wilson loop projection, right:  $S_{x,\mu}(l)$  projection, upper/lower plot: symmetric/Higgs phase  
 Figure 4: Same as Fig. 3 for second/first excited state

with [14] (the first excitation is a Higgs state, too). In the broken phase, the first excited Higgs state still contains some admixture of pure gauge matter which vanishes only deeply inside this phase. This seems to be a precursor of the near end of the transition. More details, statistics and results for other quantum numbers will be discussed elsewhere [15].

Since Wilson loops have different projection properties in both phases we have studied the flow of the mass spectrum with  $\beta_H$  or  $m_3^2(g_3^2)/g_3^4$  at  $M_H^* = 100$  GeV ( $\lambda_3/g_3^2 = 0.15625$ ) safely above the critical Higgs mass, too, passing there an analytic crossover. In Fig. 5 we present the  $0^{++}$  spectrum in the vicinity and far from the crossover. The wave functions are similar to those discussed before. Here the spectrum on the "symmetric" side shows decoupling of Higgs and  $W$ -ball states, too, the lowest  $W$ -ball mass is roughly independent on  $\beta_H$ . Passing the crossover (from "symmetric" to the "broken" side) the first Higgs excitation contains also excited glue. These contributions vanish at lower temperature as indicated by the right figure. The minimum of the ground state mass remains finite, therefore the correlation length fits into the lattice.

The phenomenological interest is now concentrated on extensions of the standard model, with MSSM being the most promising candidate. Concerning non-perturbative physics in general, however, the lattice version of the standard Higgs model remains interesting as a laboratory for investigating the behaviour of hot gauge fields coupled to scalar matter, for the characterisation of possible bound states, for the understanding of real time topological transitions and as a cross-check for analytical approximation schemes.

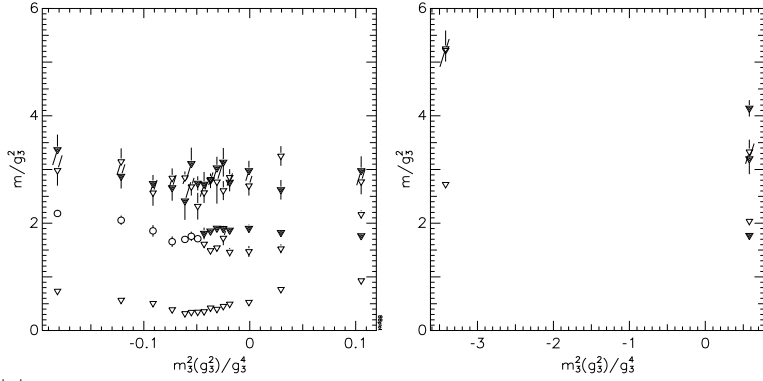


Figure 5:  $0^{++}$  spectrum beyond the critical Higgs mass; left: near to crossover, right: far from crossover. Triangles denote Higgs states, full symbols  $W$ -ball states and circles Higgs states with admixture of pure gauge matter

## References

- [1] M. Gürtler *et al.*, *Nucl. Phys. B (Proc. Suppl.)* **49**, (1996) 312
- [2] M. Gürtler *et al.*, *Nucl. Phys.* **B483** (1997) 383
- [3] K. Kajantie *et al.*, *Nucl. Phys.* **B466** (1996) 189
- [4] F. Karsch *et al.*, *Nucl. Phys.* **B474** (1996) 217
- [5] Z. Fodor *et al.*, *Nucl. Phys.* **B439** (1995) 147; F. Csikor *et al.*, *Nucl. Phys.* **B474** (1996) 421; Y. Aoki, *Phys. Rev.* **D56** (1997) 3860; F. Csikor, Z. Fodor, J. Heitger, *KEK-TH-541*(1997), hep-lat/9709098
- [6] K. Rummukainen, *Nucl. Phys. B (Proc. Suppl.)* **53** (1997) 30
- [7] M. Gürtler, E.-M. Ilgenfritz, A. Schiller, *Eur. Phys. J.* **C1**, (1998) 363
- [8] Z. Fodor, these proceedings
- [9] K. Kajantie *et al.*, *Nucl. Phys.* **B458** (1996) 90
- [10] M. Laine, *Nucl. Phys* **B451** (1995) 484
- [11] M. Gürtler, E.-M. Ilgenfritz, and A. Schiller, *Phys. Rev.* **D56**, (1997) 3888
- [12] F. Karsch *et al.*, *Nucl. Phys. B (Proc. Suppl.)* **53** (1997) 623
- [13] M. Lüscher, U. Wolff, *Nucl. Phys.* **B339** (1990) 222; C.R. Gatttringer, C.B. Lang, *Nucl. Phys.* **B391** (1993) 463
- [14] O. Philipsen, M. Teper, H. Wittig, *Nucl. Phys.* **B469** (1996) 445; *OUTP-97-44-P*, hep-lat/9709145
- [15] M. Gürtler, E.-M. Ilgenfritz, A. Schiller, C. Strecha, in preparation